

2015

Secondary Electron Yield of Electron Beam Welded Areas of SRF Cavities

M. Basovic

Old Dominion University

S. Popovic

Old Dominion University, spopovic@odu.edu

M. Tomovic

Old Dominion University, mtomovic@odu.edu

L. Vuskovic

Old Dominion University, lvuskovi@odu.edu

A. Samolov

See next page for additional authors

Follow this and additional works at: https://digitalcommons.odu.edu/physics_fac_pubs

 Part of the [Engineering Physics Commons](#), and the [Plasma and Beam Physics Commons](#)

Repository Citation

Basovic, M.; Popovic, S.; Tomovic, M.; Vuskovic, L.; Samolov, A.; and Cuckov, F., "Secondary Electron Yield of Electron Beam Welded Areas of SRF Cavities" (2015). *Physics Faculty Publications*. 272.

https://digitalcommons.odu.edu/physics_fac_pubs/272

Original Publication Citation

Basovic, M., Čučkov, F., Popović, S., Samolov, A., Tomovic, M., & Vušković, L. (2015). Secondary Electron Yield of Electron Beam Welded Areas of SRF Cavities. In *Proceedings of the 17th International Conference on RF Superconductivity (SRF2015)*, Whistler, BC, Canada, Sept. 13-18, 2015 (pp. 196-200).

Authors

M. Basovic, S. Popovic, M. Tomovic, L. Vuskovic, A. Samolov, and F. Cuckov

SECONDARY ELECTRON YIELD OF ELECTRON BEAM WELDED AREAS OF SRF CAVITIES

M. Basovic, S. Popovic, M. Tomovic, L. Vuskovic, Center for Accelerator Science, Old Dominion University, Norfolk, VA 23529, USA

A. Samolov, F. Cuckov, Department of Engineering, University of Massachusetts, Boston, MA 02125, USA

Abstract

Secondary Electron Emission (SEE) is a phenomenon that contributes to the total electron activity inside the Superconducting Radiofrequency (SRF) cavities during the accelerator operation. SEE is highly dependent on the state of the surface. During electron beam welding process, significant amount of heat is introduced into the material causing the microstructure change of Niobium (Nb). Currently, all simulation codes for field emission and multipacting are treating the inside of the cavity as a uniform, homogeneous surface. Due to its complex shape and fabricating procedure, and the sensitivity of the SEE on the surface state, it would be interesting to see if the Secondary Electron Yield (SEY) parameters vary in the surface area on and near the equator weld. For that purpose, we have developed experimental setup that can measure accurately the energy distribution of the SEY of coupon-like like samples. To test the influence of the weld area on the SEY of Nb, dedicated samples are made from a welded plate using electron beam welding parameters common for cavity fabrication. SEY data matrix of those samples will be presented.

INTRODUCTION

Intrinsic quality factor (Q factor) is a measure of quality of Superconducting Radiofrequency (SRF) cavities. Q factor is highly dependent of the state of the cavity surface and therefore all fabrication and preparation processes are having an effect on the final shape of the Q factor curve. Impurities and defects are introduced to Niobium (Nb) surface during fabrication and preparation process and are added to the previously existing impurities of Nb sheet metal. Most of the imperfections of the surface are introduced during forming and welding of the half cells. Performance of the cavities is reduced due to the presence of these surface imperfections and is limiting the overall performance of linear accelerators. In order to mitigate the influence of surface irregularities and improve the operation, cavities are subjected to an extensive etching and cleaning procedure [1]. This procedure has had a great success in increasing the maximum achievable accelerating gradient [2]. Regardless of the all surface processing so far, theoretical accelerating gradient maximum for Nb is yet to be achieved [3]. In ideal case, accelerating cavities are under perfect vacuum allowing only presence of accelerated particles. In real case, combination of imperfect vacuum, cavity surface irregularities, and presence of high electric and magnetic fields provide the

initial number of free particles and the means for their multiplication. Phenomenon which describes the multiplications of free charged particles inside the cavity is called Secondary Electron Emission (SEE). At high accelerating gradients main power losses in the cavities are due to field emission [4] and multipacting [5]. Magnetic and electric field confined inside the cavity can accelerate free particles toward the surface. Due to the impact more free electrons can be released into vacuum causing a net increase in the number of free charged particles. The magnitude that describes the SEE is called Secondary Electron Yield (SEY). SEY is defined as the number of emitted electrons per impacting electron. If the value of SEY is larger than one, buildup of free particles will cause the increasing power losses, leading to the “quenching” of cavity.

Manipulating the SEY curve of a material has been a research topic ever since the discovery of SEE. Depending on the application goal can be to increase or decrease the SEY values of the material. Magnitude of the SEY is a function of the impacting electrons [6] and the angle at which they are impacting the surface [7]. For cavities and beam tubes research has been conducted towards the reducing the SEY magnitude of the used material. Several methods have been developed and used for decreasing the value of SEY. Some of those methods include surface coatings [8], baking [9], exposure to glow discharge [10], and electron beam irradiation [6].

Multipacting and field emission simulation codes are currently modeling the cavity as uniform homogeneous structure with uniform properties of SEY across its surface. Based on the research showing the effect of baking on SEY and the fact that during welding amount of heat induced in material is changing its microstructure in an area of the weld, we believe that it is important to determine if and to what extent the SEY has changed in the area of weld.

Accelerating cavity is a very complex structure to fabricate. During the fabrication process of cavities is when the majority of the surface impurities are introduced. Joining of cavity half cells is performed by electron beam welding. Significant amount of heat is induced in material during the process causing the microstructure changes in the area of and close to welding. Three separate microstructures can be observed in the weld area of equator and iris [11, 12]. At the equator, weld zone is formed from melted Nb during welding process. This zone has a distinct microstructure. Heat affected zone is found on both sides of the weld zone and formed during welding but without melting of

Nb. Microstructure in this area varies from increased grain size on the weld zone side to grain size similar to the base metal. After heat affected zone, heat has dissipated enough not to cause any further change in initial microstructure.

EXPERIMENTAL SETUP

An experimental setup has been developed to examine the variation of the SEY on characteristic surfaces of accelerating cavities. Details of the experimental setup have been presented elsewhere [13].

SAMPLE FABRICATION AND PREPARATION

The experimental setup has been designed to hold the coupon-like samples of 20 mm in diameter and 3 mm thickness. Dimensions of the sample have been chosen in order to best represent the bulk Nb sheet metal used for cavity fabrication. Two different types of samples have been fabricated. Samples have been cut from a sheet metal with water jet machine in order to mitigate the surface changes to the sample due to inducted heat that is present in more conventional cutting techniques. Water jet cutting has been performed by Chesapeake Bay Rubber and Gasket. The first type represents the bulk of the cavity surface. Material for this type of samples has been provided by Jefferson Lab. The second type is made to replicate the weld joint on the cavity. Two sheet metal plates of Nb have been prepared for welding. Welding parameters used to join the plates are same as for cavity welding. Electron beam welding has been performed by Jefferson Lab. Width of the weld zone is approximately 4 mm. After welding, sample has been cut by water jet so that the weld is located along the diameter of the sample. Material for the second sample has been purchased from Eagle Alloys Corporation. Before the samples are mounted on the specimen stage, they have been cleaned in the ultrasonic cleaner for 3 hours to remove any surface impurities present from material handling.

MEASUREMENT PARAMETERS AND ELECTRON BEAM CONTROL

Before the test measurements can be performed vacuum level of $3 \cdot 10^{-9}$ Torr must be achieved to ensure the measurement stability. During the electron gun operation vacuum level does not exceed $3.5 \cdot 10^{-9}$ Torr. Distance of the sample from the mouth of the electron gun is set to be 25 mm. Electron gun used to provide the beam is ELG-2 manufactured by Kimball Physics. Energy range of the electron gun goes from 1 eV to 2 keV. Power supply used is EGPS-1022E from the same manufacturer. Electron gun and power supply are controlled remotely by the use of LabView software and two National Instruments PCI cards, 6034E and 6317. Current measurement is done by using Keithley 6482 dual channel picoammeter. Current is measured at two different locations in the experimental setup. One channel of the picoammeter is used to measure

the current on the sample (i_s) while the other channel is used to measure the current on the collector (i_c). The sum of these two currents (i_p) represents the primary electron beam current,

$$i_p = i_s + i_c. \quad (1)$$

Parameters of the electron gun used to obtain a controlled electron beam are: Source voltage 1.1 V, Grid voltage 16 V, and 1st Anode voltage 93 V. Once the Source voltage is set, waiting period of at least two hours is necessary while the current of the filament can stabilize. Grid and 1st Anode voltages are parameters used to control the amount of electrons that are reaching the sample. Grid voltage is reducing the measured current while 1st Anode is increasing it. By combining these two values we can set the specific primary electron beam current. To set the primary electron beam current, electron energy is set to 400 eV and Grid and 1st Anode voltages are set so that the i_p is around 520 pA. It has been observed that during each start-up of the electron gun this current at set parameters varies by a small amount.

The next parameter that needs to be controlled is the beam size. Electron gun parameter that controls the beam size is Focus voltage. Size of the electron beam is a function of all parameters we have set so far and electron energy as well. Most common way of determining the size of the electron beam is by using the phosphor screen. Unfortunately, at low currents phosphor screen we used was not sensitive enough to determine the electron beam size. We needed to develop our own device that will allow us to determine the size of the electron beam even at low energy and low currents. One of the limitations of the device was its size which could not be larger than the sample diameter. It also needed to be mounted on the specimen stage to avoid making any significant changes to the experimental setup. We have adopted the approach used in [14]. The device collector consists of the back plate, Teflon insulator, and front plate. We are calling this device primary beam collector. Back plate and front plate are made of stainless steel. Front plate has two holes in it, one 2 mm in diameter and the other 3 mm. Hole sizes are chosen based on the width of the weld zone on the sample we fabricated. Two channels of the picoammeter were connected to the front plate and the back plate. The ratio of electron currents (A) passing through a specific hole is calculated as a ratio of the back plate current and sum of the front plate and the back plate current,

$$A = \frac{i_{BP}}{i_{FP} + i_{BP}} \leq 1. \quad (2)$$

To prevent the influence of secondary and tertiary electrons on beam size measurement all components along the electron beam path have to be positively biased. In this case, our collector bias was 25 V, front plate bias

was 30 V, and back plate bias was 50 V. These voltage levels are high enough to prevent the majority of secondary electrons (SE) from leaving the surface of their respective components, but low enough not to interfere with electron beam traveling through them. After setting the electron gun to previously mentioned parameters we started varying energy of the primary electrons and adjusting the focus voltage to achieve the required beam size. Due to the bias voltages used to prevent SE from leaving the surface, our energy measurements start at 60 eV. We ranged the energy from 60 eV to 400 eV by 20 eV increments, then from 400 eV to 1500 eV by 50 eV increments, and from 1500 eV to 2000 eV by 100 eV increments. The optimal focus voltage for each energy is recorded and the functions is presented (see Fig. 1).

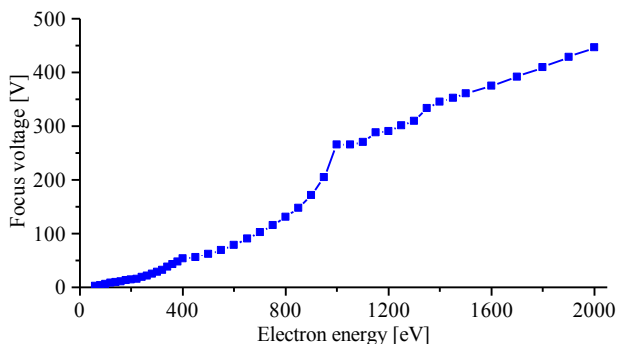


Figure 1: Focus voltage of the electron gun as a function of electron energy.

Determining the size of the beam using this technique only indicates the amount of electrons going through the specific hole on the front plate. The ratio of electron currents passing through both 2 mm and 3 mm holes are given in Fig. 2.

To determine the measurement parameters of the voltage bias on the collector and the sample we have performed multiple measurements at 100, 200, 300, and 400 eV of primary electron energy. At each energy level, voltage on the collector was varied from 0 V to +50 V. For every voltage value on the collector we also varied sample voltage from 0 to -50 V. For every electron energy SEY was determined using

$$SEY = \frac{i_c}{i_p} = \frac{i_c}{i_c + i_s}. \quad (3)$$

We have found that the primary electron beam current is almost constant with very small variations for each combination of collector and sample voltage bias. Also, we have determined that past +30 V of collector bias, SEY values stabilizes for each tested energy level. Similar statement can be made for sample bias of -10 V. Positive bias on the collector is necessary to capture all incoming SE as well as prevent the formation of tertiary electrons on the collector surface. Negative bias on the sample prevents the emitted SE to travel back to the surface of

the sample. Based on these results we have selected the collector bias level at +30 V and sample at -10 V for our measurement parameters.

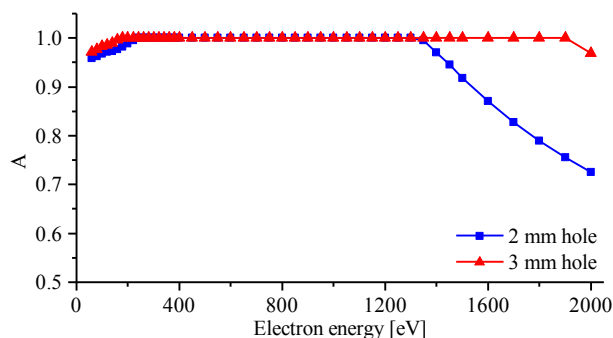


Figure 2: The ratio of electron currents A as a function of electron energy. The size of the front plate hole is indicated.

In order to verify the validity of Eq. 1 we have used the primary electron beam collector to measure the current of the focused primary beam at several different voltages of back plate starting from initial 50 V to 120 V which was the limit of the power supply used. Front plate and collector bias were kept at constant 30 V and 25 V, respectively. Primary electron beam current was measured at 200, 400, 800, and 1000 eV. Current was first measured at back plate and front plate. Then, current was measured back plate and the collector. We compared the currents at the back plate for both measurements and the results are almost a complete match. Currents measured on front plate and collector were 2 orders of magnitude less than the current on the back plate. For the next step in validating Eq. 1, we have replaced the primary beam collector with the Nb sample. Collector bias was kept at +25 V, while the sample bias was varied from +50 V to +120 V. In this measurement we have found that the sample current was higher than the back plate current. But also there was an increase in collector current as well. This can be explained by the fact that the energies at which we were performing the measurements are always higher than the bias level. Those electrons with energies higher than bias level can travel between the sample and the collector unaffected by their respective fields. Algebraic sum of the sample and collector current matches with the current measured on the back plate. When these two measurements of the primary electron beam current are compared to the current taken during the SEY measurements of the samples we can conclude that they are in good agreement.

MEASUREMENT OF THE SEY

Our initial test measurements have been performed on three samples. Nb samples 1 and 2 used corresponds to the first type of samples discussed previously. Nb sample 1 has been used for all test measurements performed so far. It has been exposed to various beam current magnitudes as well as different beam spot sizes. Exposure

time to beam with various parameters can be measured in hours. Sample has been repeatedly exposed to air during the development of the experimental setup and then reconditioned with electron beam after each pump down. With that in mind we cannot make any claims on the initial or current state of the sample surface. Nb sample 2 is same as the Nb sample 1 except that it has not been exposed to electron beam at all. Nb sample 1 and 2 are made from a plate provided by Jefferson Lab. Sample 3 corresponds to the second type of samples already described. This sample contains weld joint on its surface. It has been cut by a water jet and degreased in ultrasonic cleaner prior to the mounting on the specimen stage. This sample will be denoted as Weld joint Nb sample to differentiate it from previous two samples. During the electron gun parameter search and measurements this sample was not exposed to electron bombardment. Electron beam was directed at the weld zone of this sample to determine the SEY of that particular area. Weld joint Nb sample is made from Eagle Alloys plate. These three samples are used as the initial test measurement of the experimental setup and as a starting point for further investigation of Nb SEY.

From this point, all three samples have undergone the same number of measurements and the same schedule of measurements. There have been total of seven different measurements performed on all samples, on three different days. Measurements have been performed in the same energy range and increments used when the Focus voltage function was determined. On the first day, two consecutive measurements have been performed on each sample. We started at 60 eV and finished at 2000 eV energy on both measurements of each sample. Same schedule was repeated on the second day. On the third day, three consecutive measurements have been performed. The first and the second measurement was performed backwards from 2000 eV to 60 eV to determine whether the electron beam is warming sample and if that changes the SEY curve significantly. The third measurement has been performed in the same manner as in previous days. We have found no significant changes in the SEY curve between forward and backward measurement of SEY.

RESULTS

In Fig. 3, we have plotted the average curve of primary electron beam current for each of the samples. Corresponding average SEY curves are presented for tested samples in Fig. 4. Averages have been taken based on seven measurements performed on each sample. Statistical error bars have been calculated using t-distribution and small sample size correction, which in this case is seven. Error bars are covering 95% confidence level of the results.

There are two characteristic parts of primary electron beam curve in Fig. 3. First part occurs for energies from 60 eV to 500 eV. Primary electron beam current variations in the energy range from 60 to 160 eV is larger than the rest of the curve. Past 160 eV

variation in current stays almost constant up to maximum electron energy. Second part of the primary electron beam current curve is characterized by a very small slope and slow linear increase in current. Differences in error bars between samples can be explained by the fact that for Nb sample 1 SEY measurements are performed right after the warm-up period of the electron gun, while the Weld joint Nb sample SEY measurements were done last for each day. This is probably due to fact that the current is much more stable after longer time periods of electron gun operation. Increasing the warm-up period of electron gun will probably lead to smaller differences in primary electron beam current during one operating cycle. If we take a look at the Nb sample 1 SEY curve we can see that even with the larger variation of current results are not affected in a significant way. For the Weld joint Nb sample SEY curve has much higher error bars even with the much more stable primary electron beam current. This leads us to conclude that variations of current between the measurements and during the measurements are not affecting the SEY measurements in a significant manner. Across the whole energy range for each of the measurements performed difference between the lowest and highest current value does not exceed 140 pA.

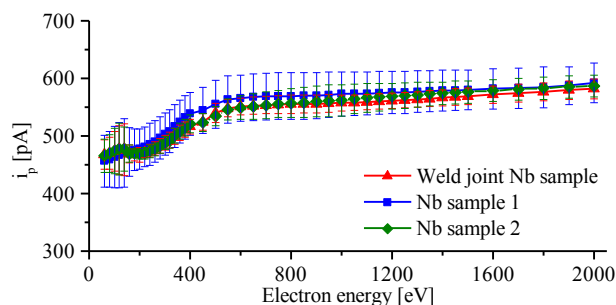


Figure 3: Primary electron beam current as a function of electron energy during SEY measurement of Nb sample and weld joint Nb sample. Statistical error bars are indicated.

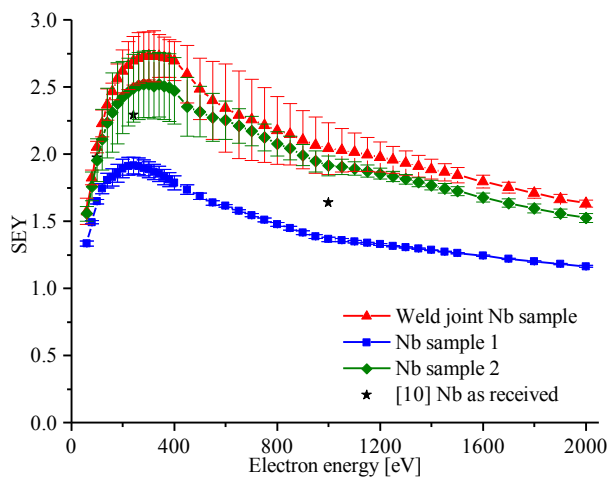


Figure 4: Preliminary results of SEY as a function of electron energy for Nb samples 1 and 2, and Weld joint Nb sample. Statistical error bars are indicated.

The SEY curve of the Nb sample 1 is very constant for each of the measurements performed. Stability of the results on this sample can be explained by the fact that this sample was exposed to various beam currents at longer periods of time. Highest variations in SEY curve are occurring in the energy range from 100 eV to 400 eV. In the most extreme case of that range, yield is varying up to 10%. For energies above 400 eV variations of SEY values are almost negligible.

SEY curve of Nb sample 2 has much larger variation due to unconditioned surface of the sample. After each measurement SEY curve was lower than the previous. Variations in the yield results are the largest from 100 eV to 400 eV. After 1000 eV variations are minimal.

The SEY curve of Weld joint Nb sample shows much larger variation between measurements. With each measurement SEY curve was overall becoming lower. Because the surface of the sample was not exposed to electron beam prior to the set of measurements taken this can be expected, based on the published research [7]. What we found very interesting is that different parts of the SEY curve have different rate of SEY reduction. From the error bars of Weld joint Nb sample in Fig. 4 we can see that from 450 eV to 900 eV reduction in SEY change was larger in magnitude compared to the rest of the SEY curve. Second part of the SEY curve that has significant change in SEY magnitude is from 60 eV to 400 eV. In the range from 1400 eV to 2000 eV changes in SEY are much smaller after all measurements than in the other sections of the curve.

CONCLUSION

We have developed and tested the experimental setup for measurement of the SEY of coupon-like samples. Initial results, even though not definitive, have given us a reason to pursue this avenue of research. Measurements of the SEY on Weld joint Nb samples have shown higher SEY compared to the Nb samples 1 and 2. Due to the different histories of the samples used for testing, we cannot make any definitive claims about the results presented here. These results are just initial measurements used to test the developed experimental setup, selected measurement parameters, and electron beam control. To reduce the variability between the samples we will fabricate several sets of samples of both types from a single plate. By reducing the variability between the samples we are hoping to show what effect welding has on the SEY of Nb. Our plan is to measure the effect of incident angle of electron beam to the sample surface on SEY of both regular and welded samples, as well. We also plan to include the measurement of SEY in the heat affected zone of the welded sample. For the next step in the experiment, we will test the influence of plasma treatment on SEY for different microstructures in weld area of Nb, as well as different incidence angles. These measurements will also be performed on both types of samples. Our goal is to characterize the changes in the SEY of Nb in the weld regions of accelerating cavities.

ACKNOWLEDGEMENTS

Thomas Jefferson National Accelerator Facility, Accelerator Division supports M. Basovic through fellowship under JSA/DOE Contract No. DE-AC05-06OR23177.

REFERENCES

- [1] B. Aune, *et.al.*, "Superconducting TESLA cavities", Phys. Rev. ST – Accelerators and Beams **3**, 092001 (2000).
- [2] L. Lilje, *et.al.*, "Improved surface treatment of the superconducting TESLA cavities", Nucl. Instrum. Methods A **516**, 213 (2004).
- [3] K. Saito, "Critical field limitation on the Niobium superconducting RF cavity", 10th Workshop on RF Superconductivity, Tsukuba, Japan (2001).
- [4] J. Knobloch, "Field emission and thermal breakdown in superconducting Niobium cavities for accelerators", IEEE Trans. on Applied Superconductivity **9**, 1016 (1999).
- [5] J. R. M. Vaughan, "Multipactor", IEEE Trans. Electron Devices **35**, 1172 (1988).
- [6] R. Larciprete, D. R. Grosso, M. Commisso, R. Flammini, R. Cimino, "Secondary electron yield of Cu technical surfaces: Dependence on electron irradiation", Phys. Rev. ST – Accelerators and Beams **16**, 011002 (2013).
- [7] H. Bruining, "Secondary electron emission", Physica **V**, 10 (1938).
- [8] B. Henrist, N. Hilleret, C. Scheuerlein, M. Taborelli, "The secondary electron yield of TiZr and TiZrV non-evaporable getter thin film coatings," Applied Surface Science **172**, 95 (2001).
- [9] V. Baglin, J. Bojko, O. Grobner, B. Henrist, "The Secondary Electron Yield of Technical Materials and Its Variation with Surface Treatments", Proc. EPAC, Vienna (2000).
- [10] R. Calder, G. Dominichini, N. Hilleret, "Influence of Various Vacuum Surface Treatments on the Secondary Electron Yield of Niobium", Nucl. Instrum. Methods B **13**, 631 (1986).
- [11] C. A. Cooper, L. D. Cooley, "Mirror-smooth surfaces and repair of defects in superconducting RF cavities by mechanical polishing", Superconducting Science and Technology **26**, 015011 (2013).
- [12] R. L. Geng, J. Knobloch, H. Padamsee, "Microstructures of RF surfaces in the electron-beam-weld regions of Niobium", Proc. 9th Workshop on RF Superconductivity, Santa Fe (1999).
- [13] M. Basovic, A. Samolov, F. Cuckov, S. Popovic, M. Tomovic, L. Vuskovic, "Effects of plasma processing on secondary electron yield of Niobium samples", Proc. IPAC 2015, Richmond (2015).
- [14] W. H. Hartung, *et.al.*, "In-situ measurements of the secondary electron yield in an accelerator environment: Instrumentation and methods", Nucl. Instrum. Methods A **783**, 95 (2015).